

On the interpretation of spin-polarized electron energy loss spectra

R. Saniz

Departamento de Ciencias Exactas, Universidad Católica Boliviana, Casilla #5381, Cochabamba, Bolivia

S. P. Apell

Department of Applied Physics, Chalmers University of Technology and Göteborg University, S-41 296, Göteborg, Sweden

(March 3, 2000)

We study the origin of the structure in the spin-polarized electron energy loss spectroscopy (SPEELS) spectra of ferromagnetic crystals. Our study is based on a 3d tight-binding Fe model, with constant onsite Coulomb repulsion U between electrons of opposite spin. We find it is not the total density of Stoner states as a function of energy loss which determines the response of the system in the Stoner region, as usually thought, but the densities of Stoner states for only a few interband transitions. Which transitions are important depends ultimately on how strongly umklapp processes couple the corresponding bands. This allows us to show, in particular, that the Stoner peak in SPEELS spectra does not necessarily indicate the value of the exchange splitting energy. Thus, the common assumption that this peak allows us to estimate the magnetic moment through its correlation with exchange splitting should be reconsidered, both in bulk and surface studies. Furthermore, we are able to show that the above mechanism is one of the main causes for the typical broadness of experimental spectra. Finally, our model predicts that optical spin waves should be excited in SPEELS experiments.

75.25.+z, 75.30.Ds.

I. INTRODUCTION

The study of elementary excitations in itinerant-electron ferromagnets is an area which is currently very active in spite of the enormous amount of publications on the subject since early work in the sixties (see e.g. Refs. [1,2] and references therein). From the beginning, experimental and theoretical work on these materials concentrated on neutron scattering and dynamical susceptibility studies. [1,3–6] Efforts have continued in this direction until today, both because of the gradual improvement of electronic band structure calculations [7,8] and because of the improvement of the experimental method. [9] Around the mid-eighties, however, a new technique was introduced in the field, namely, spin polarized electron energy loss spectroscopy (SPEELS). Among its first successes, one can count the first observations, in a ferromagnetic glass [10] and in nickel, [11] of what were interpreted as Stoner excitations. Further work, reporting more detailed measurements, confirmed those findings. [12,13] Theoretical model calculations of inelastic electron spin-flip exchange scattering, [14–17] provided a basis for the interpretation of those observations in terms of Stoner excitations. In addition, Vignale and Singwi found in their work that spin waves should also be observable in SPEELS measurements. [16] However, these had not been observed at the time, nor were they observed in the several years that followed. Spin waves were found in other model calculations, [18,19] the calculations of Plihal and Mills being the most conclusive in this respect because of their more accurate treatment of electronic structure. [19] It is only very recently that the detection of spin waves in a SPEELS experiment has finally been reported. [20] The application of SPEELS has been naturally extended to the study of magnetic surfaces. [21–23] An important theoretical effort in this direction is that by Mills and collaborators, [24–26] who have studied ferromagnetic thin films as well.

To introduce the questions addressed by this work, we recall briefly some of the main concepts involved in SPEELS and discuss some of the findings to date. SPEELS is a spin-polarized version of electron energy loss spectroscopy in the sense that the spin polarization of the scattered electrons is also measured. The impinging electron often is also spin-polarized, but this is not necessarily so (see e.g. Refs. [10,11]). In a so-called spin-flip exchange scattering event, an incoming electron with given spin comes to occupy an empty level in the material while an electron with opposite spin is driven out and is detected. The process produces thus a Stoner excitation. In the band picture of magnetic transition metals, below the Curie temperature, the exchange split $3d$ bands provide large densities of occupied majority-spin states below the Fermi energy and vacant minority-spin states above it. Thus, it is more likely for an impinging electron with minority spin to excite a Stoner pair than for a majority-spin incoming electron, particularly for an ex-

citation energy corresponding to the exchange splitting of the ferromagnet. This is the mechanism invoked to explain the Stoner peak or the asymmetry reported in Refs. [10] and [11] and further experimental work (Refs. [12,13]). However, it turned out necessary to elaborate on several other issues. Firstly, the Stoner peak was very broad in all observations. This was interpreted by Kirschner, Rebenstorff, and Ibach [11] as an indication of the nonuniformity of exchange splitting throughout the Brillouin zone. Then, in Fe, the energy loss at which the Stoner peak occurs and its width were reported by Venus and Kirschner to increase with increasing scattering angle, [12] a fact that was correlated by these authors with the calculated density of Stoner states. Also, a threshold for the onset of Stoner excitations in Ni(110) was reported by Abraham and Hopster [13] and interpreted in terms of the Ni $3d$ band structure. These workers, moreover, indicated that their spectra did not differ significantly for off specular scattering angles ranging from 10° to 40° , [27] which they explained as due to the non-conservation of the momentum component perpendicular to the surface.

Finally, an important application based on SPEELS interpretation is that, in surface and thin film studies, the Stoner peak is assumed to give information on the surface magnetic moment through the correlation between exchange splitting and moment. [22,23] In particular, a Stoner peak found at higher energies than the exchange splitting bulk value is assumed to indicate an enhanced magnetic moment at the surface.

Clearly, more theoretical work is required, for the bulk as much as for surfaces, to make further progress. In particular, it would be important to understand better the phenomenology of SPEELS and to try to be more specific about the information we can expect from it. This would also provide experimenters with useful feedback. Accordingly, we think it is worthwhile going back to a model calculation and look more closely at the dynamic properties of the material probed by SPEELS. In this work we consider a model of Fe based on paramagnetic tight-binding $3d$ bands, with up and down spin bands rigidly split. The cross section for spin-flip exchange scattering processes is evaluated within the random phase approximation, assuming the solid is described by a multi-band Hubbard Hamiltonian. As we shall see, this allows us to show that it is not the total density of Stoner states as a function of energy loss and momentum transfer which causes the structure in the Stoner region of the spectrum, but the density of Stoner states for a few interband excitations. Which interband excitations are important is essentially determined by the weight of the matrix elements for such processes. It is in this regard the contribution of umklapp scattering is fundamental because of the coupling of different bands at different energy ranges. This gives rise to a richer structure in the Stoner region of the spectra. Also, our model predicts that optical spin waves should be observable through SPEELS. Again umklapp scattering proves critical, providing optical spin waves with the

necessary oscillator strength. We find this strength to depend importantly on scattering angle.

Section II of this paper is devoted to theory, presenting the derivation of the spin-flip exchange scattering cross section for our model. We present our main results in Section III. Then follows in Section IV a discussion of our results in the light of experimental findings and other theoretical work. Finally, in Section V we summarize our work and give some conclusions.

II. THEORY

A. Spin-flip exchange scattering cross section

The electron spin-flip exchange scattering differential cross section for a N -electron system target has been previously derived on general grounds by Vignale and Singwi in terms of a particle-hole excitation correlation function. [16] One has

$$\frac{d^2\sigma}{dE d\Omega} = -\frac{m^2}{4\pi^2\hbar^4} \frac{p_f}{p_i} \frac{1}{\pi} \frac{\text{Im} \chi_{\sigma_i\sigma_f}^R(\mathbf{p}_i, \mathbf{q}, E)}{1 - e^{-\beta E}}, \quad (2.1)$$

where E is the energy loss, Ω is the solid angle, m the electron mass, and $\beta = 1/k_B T$. Momentum transfer is given by $\mathbf{q} = \mathbf{p}_i - \mathbf{p}_f$, with \mathbf{p}_i and \mathbf{p}_f the momentum of the incoming and outgoing electrons, respectively. Likewise, σ_i is the spin of the impinging electron and σ_f that of the scattered one. The retarded function $\chi_{\sigma_i\sigma_f}^R$ can be obtained by analytic continuation of the two-particle temperature correlation function

$$\chi_{\sigma_i\sigma_f}(\mathbf{p}_i, \mathbf{q}, i\omega_n) = -\int_0^\beta d\tau e^{-i\omega_n\tau} \times \langle T_\tau [\varrho_{\sigma_i\sigma_f}(\mathbf{p}_i, \mathbf{q}, \tau) \varrho_{\sigma_i\sigma_f}^\dagger(\mathbf{p}_i, \mathbf{q})] \rangle. \quad (2.2)$$

In this equation $\omega_n = 2\pi n/\beta$ is a bosonic Matsubara frequency, T_τ is the imaginary time ordering operator, and the brackets indicate the thermodynamic average in the canonical ensemble. [28] $\varrho_{\sigma_i\sigma_f}^\dagger$ is the particle-hole creation operator

$$\varrho_{\sigma_i\sigma_f}^\dagger(\mathbf{p}_i, \mathbf{q}) = -\frac{1}{N} \sum_{j=1}^N \int d\mathbf{r} d\mathbf{r}_j e^{-i\mathbf{p}_f \cdot \mathbf{r}_j} e^{i\mathbf{p}_i \cdot \mathbf{r}} \times v(|\mathbf{r} - \mathbf{r}_j|) \psi_{\sigma_i}^\dagger(\mathbf{r}) \psi_{\sigma_f}(\mathbf{r}_j), \quad (2.3)$$

where $\psi_\sigma^\dagger(\mathbf{r})$ is the field operator creating an electron of spin σ at position \mathbf{r} and $v(r) = e^2/r$ is the Coulomb interaction between the scattered and target electrons. The sum runs over the N electrons in the target system. This expression is quite general, and could be applied equally well to a solid, an atom, or a molecule.

We now consider the N electrons in a crystal material. We write the Bloch wave function for a state with wave vector \mathbf{k} and spin σ in band n in terms of Wannier functions,

$$\psi_{n\mathbf{k}\sigma}(\mathbf{r}) = \frac{1}{\sqrt{N_0}} \sum_{\mathbf{R}} e^{i\mathbf{k} \cdot \mathbf{R}} \phi_{n\mathbf{k}}(\mathbf{r} - \mathbf{R}) \eta_\sigma, \quad (2.4)$$

where N_0 is the number of sites in the crystal and η_σ is the spin function. Denoting by $a_{n\mathbf{k}\sigma}^\dagger$ the operator creating an electron in such a state, the field operators can be expanded as $\psi_\sigma^\dagger(\mathbf{r}) = \sum_{n\mathbf{k}} \psi_{n\mathbf{k}\sigma}(\mathbf{r}) a_{n\mathbf{k}\sigma}^\dagger$. The particle-hole creation operator becomes

$$\varrho_{\sigma_i\sigma_f}^\dagger(\mathbf{p}_i, \mathbf{q}) = \sum_{nn'} \sum_{\mathbf{k}} W_{nn'}(\mathbf{p}_i, \mathbf{q}, \mathbf{k}) a_{n\mathbf{k}\sigma_i}^\dagger a_{n'\mathbf{k}-\mathbf{q}\sigma_f}, \quad (2.5)$$

where the sum in momentum space runs over the Brillouin zone and matrix element $W_{nn'}$ is given by

$$W_{nn'}(\mathbf{p}_i, \mathbf{q}, \mathbf{k}) = \frac{N_0}{V} \sum_{\mathbf{K}} \hat{v}(\mathbf{k} - \mathbf{p}_i - \mathbf{K}) \hat{\phi}_{n\mathbf{k}}^*(\mathbf{k} - \mathbf{K}) \times \hat{\phi}_{n'\mathbf{k}-\mathbf{q}}(\mathbf{k} - \mathbf{q} - \mathbf{K}). \quad (2.6)$$

Here \mathbf{K} denotes vectors in the reciprocal lattice and V is the volume of the sample. The $\hat{}$ indicates a Fourier transformed function and $*$ denotes complex conjugation. To write the last two equations we have defined $a_{n\mathbf{k}+\mathbf{K}\sigma} \equiv a_{n\mathbf{k}\sigma}$ and have exploited the periodicity of the Wannier functions in the wave vector index, i.e. $\phi_{n\mathbf{k}+\mathbf{K}\sigma} = \phi_{n\mathbf{k}\sigma}$.

B. RPA expression for a tight-binding system

We are interested in the cross section for an itinerant electron ferromagnet. We describe the system within a tight-binding approximation, thus writing the Wannier wave function for given \mathbf{k} and band index n by a linear combination of atomic orbitals φ_m

$$\phi_{n\mathbf{k}}(\mathbf{r}) = \sum_m b_{mn}(\mathbf{k}) \varphi_m(\mathbf{r}). \quad (2.7)$$

The coefficients b_{mn} diagonalize the crystal Hamiltonian and are normalized so as to define a unitary matrix. Consequently, the independent-electron Hamiltonian of the system can be written $H_0 = \sum_{n\mathbf{p}\sigma} \epsilon_n(\mathbf{p}) a_{n\mathbf{p}\sigma}^\dagger a_{n\mathbf{p}\sigma}$, where the $\epsilon_n(\mathbf{p})$ are paramagnetic band energies. We assume the interacting system is described by a multi-band Hubbard Hamiltonian. In our basis we have

$$H_I = \frac{1}{2} \frac{U}{N_0} \sum_{\substack{nn' \\ mm'}} \sum_{\sigma} \sum_{\mathbf{p}\mathbf{p}'\mathbf{q}'} c_{nm}(\mathbf{p} + \mathbf{q}', \mathbf{p}) c_{n'm'}(\mathbf{p}' - \mathbf{q}', \mathbf{p}') \times a_{n\mathbf{p}+\mathbf{q}'\sigma}^\dagger a_{m\mathbf{p}\sigma} a_{n'\mathbf{p}'-\mathbf{q}'-\sigma}^\dagger a_{m'\mathbf{p}'-\sigma}, \quad (2.8)$$

where we have defined $c_{nm}(\mathbf{p}, \mathbf{q}) = \sum_l b_{ln}(\mathbf{p}) b_{lm}(\mathbf{q})$, and U is the effective on-site Coulomb interaction for two electrons with opposite spin. The RPA evaluation of the

correlation function $\chi_{\sigma_i\sigma_f}$ defined in Eq. 2.2 is a straightforward generalization of that in previous work [18]. The response function divides naturally in two,

$$\chi_{\sigma_i\sigma_f}(\mathbf{p}_i, \mathbf{q}, i\omega_n) = \chi_{\sigma_i\sigma_f}^S(\mathbf{p}_i, \mathbf{q}, i\omega_n) + \chi_{\sigma_i\sigma_f}^{\text{MB}}(\mathbf{p}_i, \mathbf{q}, i\omega_n). \quad (2.9)$$

The Stoner or single-particle excitation contribution is given by

$$\chi_{\sigma_i\sigma_f}^S(\mathbf{p}_i, \mathbf{q}, i\omega_n) = \sum_{nn'} \sum_{\mathbf{k}} \frac{f_{n'\mathbf{k}-\mathbf{q}\sigma_f} - f_{n\mathbf{k}\sigma_i}}{i\omega_n + \epsilon_{n'\sigma_f}(\mathbf{k}-\mathbf{q}) - \epsilon_{n\sigma_i}(\mathbf{k})} \times |W_{nn'}(\mathbf{p}_i, \mathbf{q}, \mathbf{k})|^2. \quad (2.10)$$

We have introduced the occupation probability of state $n\mathbf{k}\sigma$, $f_{n\mathbf{k}\sigma} = \langle a_{n\mathbf{k}\sigma}^\dagger a_{n\mathbf{k}\sigma} \rangle$, and the single-particle energy modified by the exchange self-energy

$$\epsilon_{n\sigma}(\mathbf{k}) = \epsilon_n(\mathbf{k}) - \frac{U}{N_0} \sum_{\mathbf{p}} f_{n\mathbf{p}\sigma}. \quad (2.11)$$

Thus, in this model, spin down and spin up energy bands are rigidly split by the quantity $\Delta = U(\langle n_\uparrow \rangle - \langle n_\downarrow \rangle)$, where

$$\langle n_\sigma \rangle = \frac{1}{N_0} \sum_{m\mathbf{p}} f_{m\mathbf{p}\sigma} \quad (2.12)$$

is the average number per site of states with spin σ .

The many-body contribution is given by

$$\chi_{\sigma_i\sigma_f}^{\text{MB}}(\mathbf{p}_i, \mathbf{q}, i\omega_n) = \frac{U}{N_0} \sum_{nn'} G_{\sigma_i\sigma_f}^{nn'}(\mathbf{p}_i, \mathbf{q}, i\omega_n) \times \Gamma_{\sigma_i\sigma_f}^{nn'}(\mathbf{p}_i, \mathbf{q}, i\omega_n), \quad (2.13)$$

with the auxiliary functions $G^{nn'}$ and $\Gamma^{nn'}$ defined as follows:

$$G_{\sigma_i\sigma_f}^{nn'}(\mathbf{p}_i, \mathbf{q}, i\omega_n) = \sum_{mm'} \sum_{\mathbf{k}} \frac{f_{m'\mathbf{k}-\mathbf{q}\sigma_f} - f_{m\mathbf{k}\sigma_i}}{i\omega_n + \epsilon_{m'\sigma_f}(\mathbf{k}-\mathbf{q}) - \epsilon_{m\sigma_i}(\mathbf{k})} \times W_{mm'}^*(\mathbf{p}_i, \mathbf{q}, \mathbf{k}) b_{nm}(\mathbf{k}) b_{n'm'}(\mathbf{k}-\mathbf{q}), \quad (2.14)$$

and, considering G and Γ as vectors with coefficients indexed by nn' ,

$$\Gamma_{\sigma_i\sigma_f}(\mathbf{p}_i, \mathbf{q}, i\omega_n) = \left[1 + \frac{U}{N_0} D_{\sigma_i\sigma_f}(\mathbf{q}, i\omega_n) \right]^{-1} \times G_{\sigma_i\sigma_f}(\mathbf{p}_i, \mathbf{q}, i\omega_n), \quad (2.15)$$

where the elements of matrix D are

$$D_{\sigma_i\sigma_f}^{nn',mm'}(\mathbf{q}, i\omega_n) = \sum_{ll'} \sum_{\mathbf{k}} b_{nl}(\mathbf{k}) b_{n'l'}(\mathbf{k}-\mathbf{q}) \times \frac{f_{l'\mathbf{k}-\mathbf{q}\sigma_f} - f_{l\mathbf{k}\sigma_i}}{i\omega_n + \epsilon_{l'\sigma_f}(\mathbf{k}-\mathbf{q}) - \epsilon_{l\sigma_i}(\mathbf{k})} b_{ml}(\mathbf{k}) b_{m'l'}(\mathbf{k}-\mathbf{q}). \quad (2.16)$$

To obtain $\chi_{\sigma_i\sigma_f}^R$, analytic continuation $i\omega_n \rightarrow E + i\eta$ of the above results is straightforward. Also, results in next section are obtained in the zero-temperature limit.

III. RESULTS

Before presenting our results, there are a few details of our model we should discuss. As we said in the introduction, our Fe model is based on simple $3d$ tight-binding paramagnetic bands, i.e. we neglect sp hybridization. This has, of course, incidence on the quantitative details of the response of the system. However, we will see our results are rather general and do not depend on these details. The Wannier functions were written as a linear combination of the Fe five $3d$ atomic wave functions. The overlap integrals were calculated, up to next nearest neighbors, using the Fe atomic wave functions determined according to Griffith's prescription, [29] and a lattice constant $a = 2.87 \text{ \AA}$. [30] We have, thus, a five band model. The bandwidth was set to 4.7 eV, which corresponds roughly to the bandwidth of d electrons in Fe. [31] Exchange splitting Δ was chosen to be 2 eV, taking as reference the position of the peaks in the densities of states for up and down spins. Then, the Fermi level was fixed by the condition of having six electrons per unit cell. We show the density of states for up and down spins in Fig. 1. These exhibit the bonding and antibonding regions common to BCC materials with unfilled d shells. Once the Fermi energy is fixed we can deduce the strength of the effective Coulomb interaction U in our model from $U = \Delta/(\langle n_\uparrow \rangle - \langle n_\downarrow \rangle)$. We find $U = 0.69 \text{ eV}$, which compares very well with the energy found in other works. [32] On the other hand, bulk polarization is too high, roughly 48%, [33] reflecting the lack of hybridization with sp electrons.

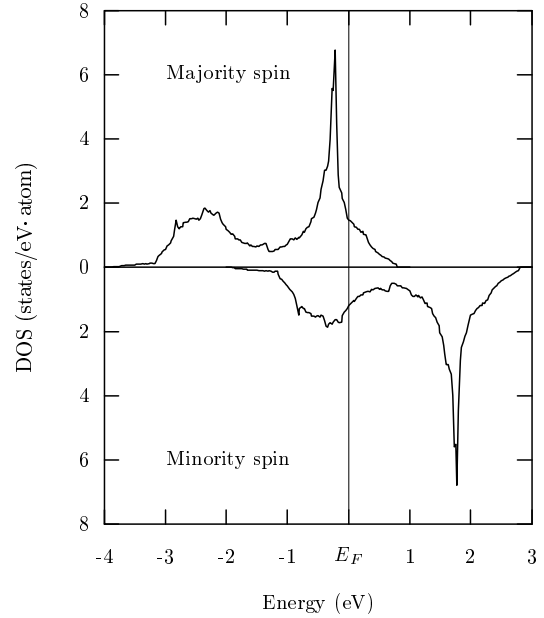


FIG. 1. The Fe up and down spin electron densities of states for our model, exhibiting the characteristic bonding and antibonding regions. Bandwidth is 4.7 eV and exchange splitting 2 eV.

In a typical SPEELS experiment, the incoming electron beam impinges on the sample surface at an angle θ to the normal and the total scattering angle is 90° . [11–13,22,23] For fixed scattering angle, i.e. for given incoming and outgoing momenta, there are three possible scattering processes corresponding to different momentum transfer. In two cases, a relatively small angle inelastic scattering event is preceded or followed by elastic scattering. In the third one, all the momentum transfer is absorbed by the electron-hole pair excitations, i.e. it is a large angle scattering event. We consider here the geometry of Venus and Kirschner, [12] that is, the sample exposes the (110) surface and the scattering plane is defined by the surface normal [110] and the [001] axis. If u is the axis normal to the surface, the three momenta mentioned are given as a function of energy loss E and impinging momentum p_i and energy E_i by

$$\begin{aligned} q_u &= p_i(\cos \theta - \sin \theta \sqrt{1 - E/E_i}), \\ q'_u &= p_i(-\cos \theta + \sin \theta \sqrt{1 - E/E_i}), \\ q''_u &= -p_i(\cos \theta + \sin \theta \sqrt{1 - E/E_i}), \\ q_z &= q'_z = q''_z = p_i(\sin \theta - \cos \theta \sqrt{1 - E/E_i}), \end{aligned} \quad (3.1)$$

where θ is the angle to the normal. The large angle scattering event corresponds to \mathbf{q}'' . Momentum transfer parallel to the surface is the same in the three cases. To calculate the final spectrum, the contributions of these three processes have to be added because experiment does not discriminate them.

Also, since Fe presents a non negligible quantity of free-like s and p states at the Fermi surface, the interaction between the incoming electrons and those in the solid will be screened. We take this into account using the Thomas-Fermi form of the screened Coulomb potential, with a screening wave vector corresponding to the density of states of s and p electrons at the Fermi surface. [34] This gives $q_{\text{TF}} = 0.26$ in units of $k_a = 4\pi/a$. Finally, an important point to mention is that we use a finite value for η when taking the analytic continuation $i\omega_n \rightarrow E + i\eta$. Since, to our knowledge, there are no estimates of the self-energy corrections for up and down spin bands in Fe, [35] we take $\eta = 80$ meV, which corresponds to the resolution in the latest experiment on this material. [20]

A. Interband densities of Stoner states

Let us consider a majority spin electron with an angle of incidence $\theta = 60^\circ$ to the normal and an incoming energy $E_i = 22$ eV, which is the energy used in Ref. [12]. We see in Fig. 2(a) that the total spin-flip exchange scattering cross section is indeed rather broad, with its peak centered at an energy much higher than the exchange splitting value (2 eV in our model), a trend observed experimentally by Venus and Kirschner [12]. We also show the partial cross sections for different momentum transfers. The curves for small scattering angle coincide for

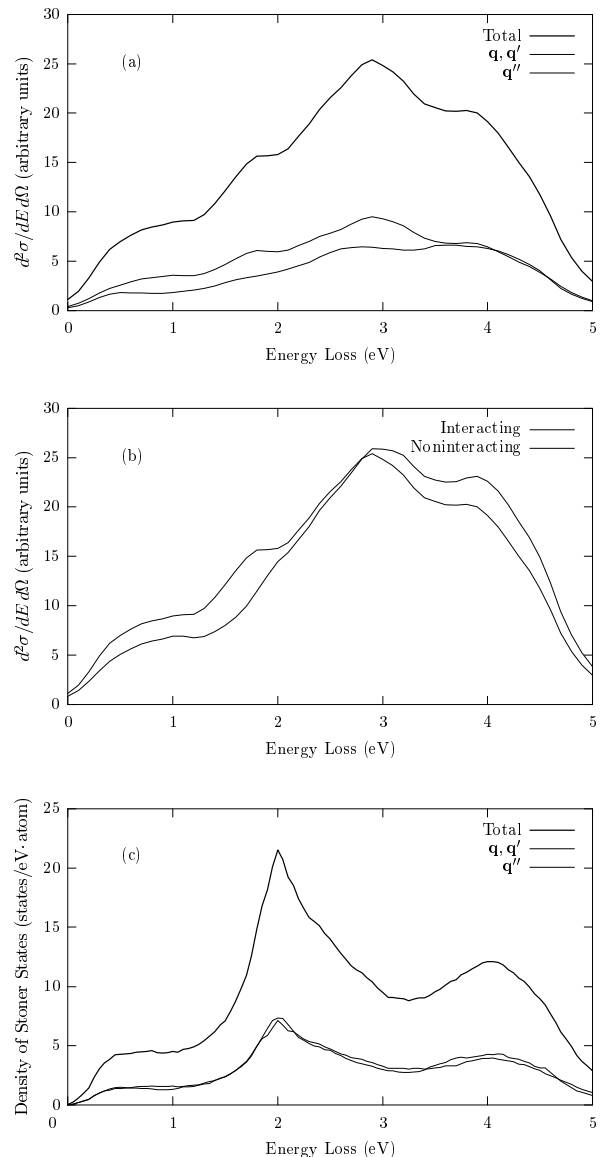


FIG. 2. (a) Spin-flip exchange cross section for a majority spin electron, with impinging energy of 22 eV and angle of incidence of 60° . We show the total cross section, as well as the partial cross sections for different momentum transfer. The peak is at 3 eV, an energy much higher than the exchange splitting $\Delta = 2$ eV. (b) Interacting and noninteracting cross sections. The difference between both curves clearly shows two collective modes, one just below 2 eV, and the other below 1 eV. The noninteracting cross section shows three distinct features, namely, the peak at 3 eV, a shoulder at 4 eV, and a broad hump around 1 eV. (c) The total and partial densities of Stoner states. These show the typical maxima at exchange splitting, which are absent from the SPEELS spectrum. The densities of Stoner states are incapable of explaining the peak of the SPEELS spectrum at 3 eV.

symmetry reasons. Though total cross section broadness is somewhat increased because of the difference between small angle and large angle scattering, the cross section

in each case is broad in itself. We have examined the origin of the structure in this spectrum. Firstly, we separated single-particle excitations and many-body effects. In Fig. 2(b) we show the noninteracting and interacting (total) cross sections. This figure clearly shows us the contributions of collective modes. Indeed, the broad feature starting around 0.2 eV indicates the excitation of low lying spin waves, and, more interestingly, the shoulder at higher energy, below 2 eV, indicates the excitation of optical spin waves. This is important because optical spin waves have not been discussed previously in connection with SPEELS measurements. We consider spin waves again further on and we concentrate here on the single particle traits. Besides the peak at 3 eV, the noninteracting cross section shows a shoulder at 4 eV and a broad feature, albeit much smaller, at low energy loss, around 1 eV or so. SPEELS spectra have often been interpreted in terms of the density of Stoner states. Accordingly, we show in Fig. 2(c) the total density of Stoner states, as well as the densities of Stoner states for different momentum transfer (as before, the curves for small angle scattering are the same). [36] It is evident in the cross sections that there is nothing reminiscent of the high density of states at the exchange splitting energy. The only features of the cross sections that can find an explanation in the density of Stoner states are the shoulder at 4 eV and, possibly, the hump around 1 eV. We have, thus, refined our study and have considered the behavior of the density of Stoner states as a function of energy loss and the bands coupled in an excitation (recall energy loss and momentum transfer are coupled, cf. Eq. (3.1))

$$\rho_{nn'}(E) = \frac{1}{N_0} \sum_{\mathbf{k}} (f_{n'\mathbf{k}-\mathbf{q}\sigma_f} - f_{n\mathbf{k}\sigma_i}) \times \delta(E + \epsilon_{n'\sigma_f}(\mathbf{k} - \mathbf{q}) - \epsilon_{n\sigma_i}(\mathbf{k})). \quad (3.2)$$

Hence, subscripts n and n' indicate minority and majority bands, respectively (bands are numbered from bottom to top). We show a plot of the density of states thus defined in Fig. 3(a). We can see that the allowed and forbidden interband excitations are completely identified (we use the term forbidden for interband excitations with vanishing density of Stoner states). Moreover, the series of Stoner peaks clearly reflect the bonding and antibonding nature of the electronic structure, giving rise to two arrays of peaks, for higher and lower excitation energies. [37] The question is, of course, which of these Stoner peaks contribute the most to SPEELS cross sections. The answer is to be found, perhaps unsurprisingly, in how strongly the different bands are coupled by the matrix elements $W_{nn'}$ of the electron-hole creation operator, which weights the contribution of each Stoner excitation (see Eq. 2.10). What is not so obvious is the outcome of the combined effect of Stoner peaks and matrix elements. Let us consider the average of the square of the absolute value of matrix elements $W_{nn'}$ over the Brillouin zone, i.e.

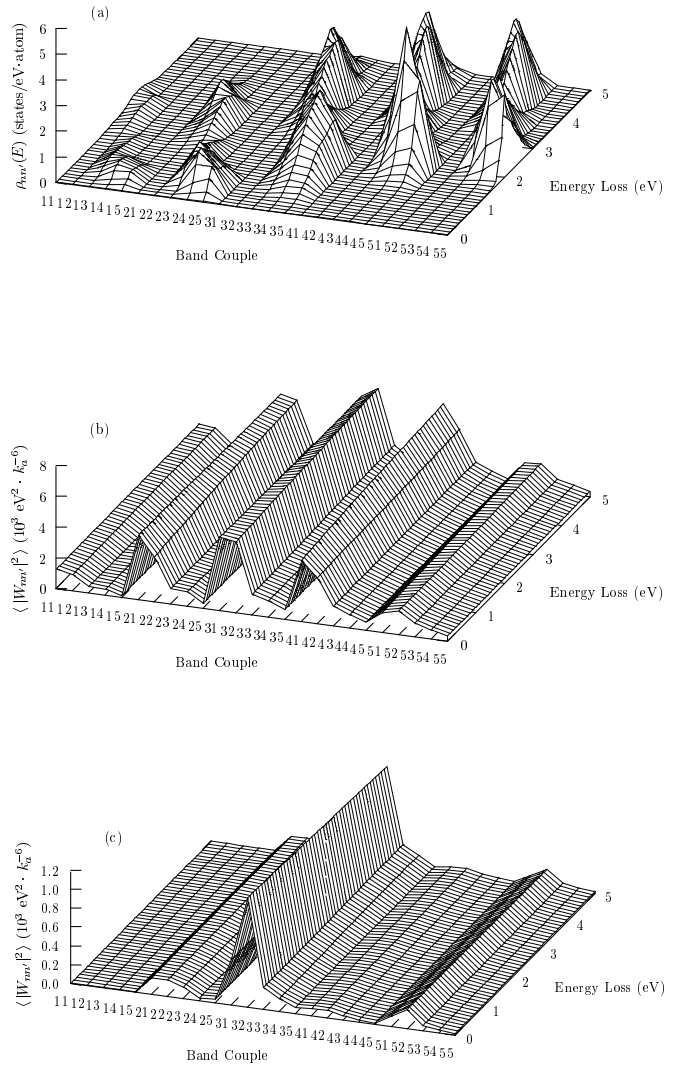


FIG. 3. (a) 3D plot of the interband densities of Stoner states. Allowed and forbidden interband excitations are clearly identified. The two series of peaks reflect the bonding and antibonding nature of the Fe electronic structure. The highest peak is found at exchange splitting, for $nn' = 44$. As we explain in the text, however, this peak contributes little to the spin-flip exchange cross section. (b) 3D plot of the average $\langle |W_{nn'}|^2 \rangle$. The slight dependence on energy results in the wave like form of the surface. The lines on the surface parallel to the energy axis correspond to fixed band couple value. The important interband excitations are determined by the crests, namely 21,22,31,32,41, and 42. One can also observe that $\langle |W_{nn'}|^2 \rangle$ reaches its lowest values for $n5$, with $n = 1, \dots, 5$. (c) 3D plot of $\langle |W_{nm}|^2 \rangle$ without umklapp processes. The important interband excitations have been reduced to $nn' = 31, 32$, thus singling out excitations in a restricted energy range.

$$\langle |W_{nn'}|^2 \rangle = \frac{1}{\hat{v}} \sum_{\mathbf{k}} |W_{nn'}|^2 \quad (3.3)$$

(\hat{v} denoting the volume of the Brillouin zone). In Fig. 3(b) we show the graph of $\langle |W_{nn'}|^2 \rangle$ as a function of energy loss and of bands coupled. There is little significant variation as a function of energy loss, but a very important structure as a function of band couple, resulting in a wave like pattern. Comparing Figs. 3(a) and 3(b) we can clearly see when it is that both quantities, $\rho_{nn'}$ and $\langle |W_{nn'}|^2 \rangle$, interfere constructively. Thus, although the density of Stoner states reaches its highest peak at exchange splitting, the average $\langle |W_{nn'}|^2 \rangle$ is negligible for the corresponding band couples. Instead, although the densities of Stoner states for interband excitations 21 and 22, 31 and 32, and 41 and 42 are more modest, the corresponding matrix element averages are high. Whence the peak around 3 eV and the shoulder around 4 eV in the noninteracting cross section in Fig. 2(b). Actually, the peak at 3 eV is more of a hat on top of the high cross section value due to interband excitations 31 and 32. We can also see that the hump around 1 eV is due to excitations coupling bands 2 and 3, and 2 and 4. To corroborate our analysis, we show in Fig. 4 the cross section taking into account solely the interband processes mentioned above. We include the total noninteracting cross section for comparison as well. We see that the few interband excitations considered indeed account almost completely for the structure of the noninteracting spectrum. An argument to understand how so simple a picture can work is that, since the atomic 3d orbitals are localized, their Fourier transform is rather flat, so that $|W_{nn'}|^2$ in the single-particle correlation function $\chi_{\sigma_i\sigma_f}^S$ (cf. Eq. (2.10)) may be replaced by its average value over the Brillouin zone. Thus, $\chi_{\sigma_i\sigma_f}^S$ is approximately proportional to $\sum_{nn'} \rho_{nn'} \langle |W_{nn'}|^2 \rangle$, a weighted average of the interband densities of Stoner states.

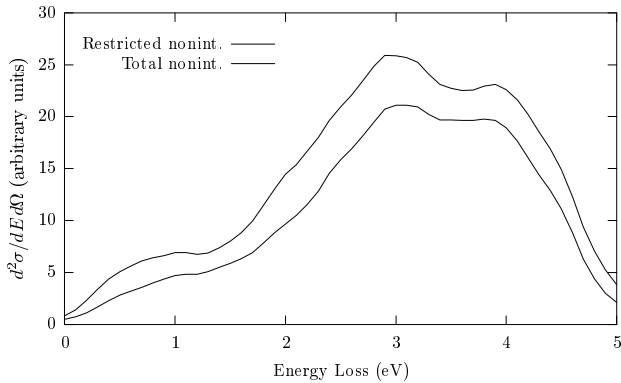


FIG. 4. Noninteracting scattering cross section taking into account only 8 ($nn' = 21, 22, 23, 24, 31, 32, 41, 42$) out of the 25 possible interband excitations, selected as explained in the text, compared to the total noninteracting scattering cross section. The first curve follows very closely to the second one.

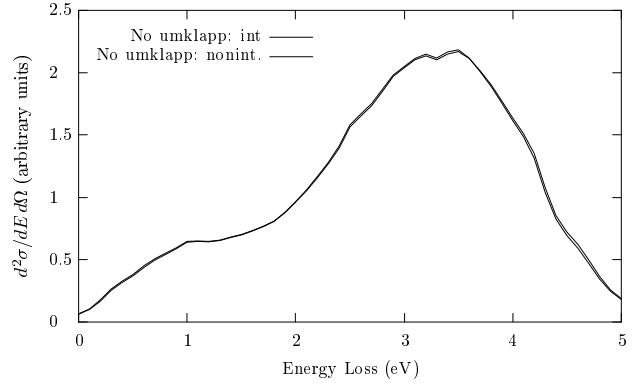


FIG. 5. Spin-flip exchange scattering cross section without umklapp processes. All that is left is a broad maximum around 3 and 4 eV, and the small hump at small energy loss. Clearly, the most important information is lost, i.e. the peak at 3 eV and the shoulder at 4 eV (cf. Fig. 2(b)).

B. Umklapp processes

Another most interesting phenomenon playing a fundamental role in SPEELS is umklapp scattering. One can see in Eq. (2.6) that the contribution of umklapp processes to the particle-hole excitation operator $\varrho_{\sigma_i\sigma_f}$ is weighted by the Coulomb interaction and the Wannier wave functions. Because of the decay of the Coulomb potential as well as of the atomic orbitals with increasing wave vector, the weight becomes rapidly negligible for lattice vectors beyond first nearest neighbors. This is enough, however, for umklapp processes to have a twofold effect. To see this, let us consider cross sections taking into account only normal excitations (i.e. with respect to the first Brillouin zone). We show this in Fig. 5, where we plot both the interacting and noninteracting cross sections. Firstly, we see that, quite apart from their much lower values in comparison with the full response case, spectra in Fig. 5 show little resemblance with those in Fig. 2(b) (scale in both figures is the same). This is because the possible interband excitations have been drastically reduced. Indeed, let us consider the graph of the average $\langle |W_{nn'}|^2 \rangle$ for excitations strictly conserving crystal momentum. We show this in Fig. 3(c). The wave crests have been reduced to that for $nn' = 31, 32$, from which it is obvious that the different wave crests in Fig. 3(b) are due to umklapp scattering. Normal scattering alone results in a spectrum almost completely distorted because of the excitation of interband transitions mainly for energies between 3 and 4 eV (cf. Fig. 3(a)).

Also, in Fig. 5 it is immediately apparent that there remains no trace of spin waves in the spectrum. Indeed, the interacting and noninteracting curves are almost indistinguishable, with no hint of the spin wave modes below 2 or 1 eV. Thus, it appears that umklapp processes provide collective excitations with oscillator strength, at

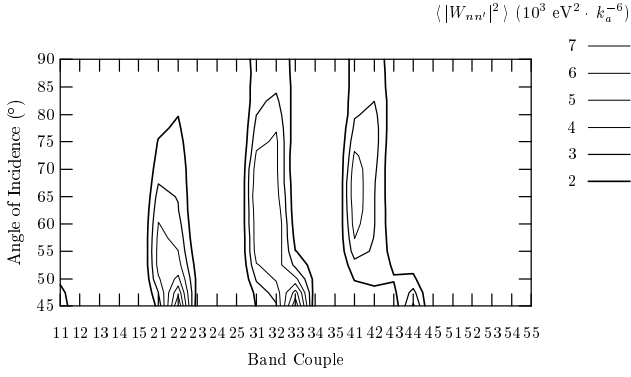


FIG. 6. Contour plot of $\langle |W_{nn'}|^2 \rangle$ as a function of scattering angle, for an energy loss $E = 2.5$ eV. Thinner lines correspond to higher averages. Drastic changes occur particularly for near specular scattering. In this case, the interband excitations for $nn' = 22, 33$ and 44 will overwhelmingly dominate the spectrum. Averages decrease significantly for large scattering angles. Comparing values for 60° and for 55° , we see that interband excitations for $nn' = 41, 42$ are less important for the latter than for the former. Similarly, for 70° , interband excitations 21 and 22 play a less important role than for 60° .

least optical modes. We must point out here that the low lying collective mode contributing to the broad feature below 1 eV is not an acoustic mode, but also an optical one. We have calculated its dispersion relation in the $[100]$ direction and found that it tends linearly to 218.7 meV for $q \rightarrow 0$. The slope is positive, but very low, with a value of $8.9 \text{ meV} \cdot \text{\AA}$. The reason is that the energy bands in our model are purely d . It is well known that models of itinerant ferromagnetism which do not take into account hybridization with sp bands, fail to describe spin waves appropriately. [38] So we do not expect our model to predict accurate dispersion relations for collective excitations. However, we do think our result properly introduces optical spin waves as a source of structure in SPEELS measurements.

C. Spectra and angle of incidence

To illustrate further the pertinence of our analysis, let us consider an example. A question addressed in the past by experimenters, without finding a clear answer, [12,13] has been that of the variation of spectra with scattering angle. Since $\langle |W_{nn'}|^2 \rangle$ plays such a consequential role, we take a look at its dependence on angle of incidence through the contour plot in Fig. 6. Generally speaking, the same interband averages remain the most important as angle changes, except toward specular scattering, when weights raise and shift significantly (then the highest values are to be found for $nn' = 22, 33$, and 44). Let us consider the spectra for angles of incidence $\theta = 55^\circ$ and $\theta = 70^\circ$. In the first case, Fig. 6 shows us that the importance of interband excitations

$nn' = 41, 42$ is diminished with respect to the $\theta = 60^\circ$ case. For $\theta = 70^\circ$, it is band couples $nn' = 21, 22$ that are diminished. In this way, in fact, we hinder the contribution of umklapp processes coupling different bands. Regarding the densities of Stoner states, on the other hand, we found that changes from one angle to another are rather small, affecting essentially only the height of the peaks. This is because a change in angle will not change the energies at which there can be a Stoner excitation, but basically the number of these. Thus, considering the averages $\langle |W_{nn'}|^2 \rangle$, the scattering cross section for 55° should present almost no shoulder around 4 eV, since interband excitations 41 and 42 are weak for that angle. Likewise, we expect the scattering cross section for 70° to have a weaker peak around 3 eV, because of the negligible contribution of excitations for $nn' = 21, 22$. We can appreciate these effects in Fig. 7. Thus, given the peaks of the interband densities of Stoner states, the shift in the Stoner excitation maximum with varying scattering angle obeys to which interband excitations receive more weight, according to the corresponding matrix elements averages. This, in turn, depends on which umklapp processes gain more importance. Fig. 7 also shows that the maximum shift causes the broadness of the spectrum to increase with scattering angle.

Turning to spin waves, it is interesting to note that the strength of the higher optical mode decreases with scattering angle. Thus it appears that umklapp scattering is unable to transmit to it sufficient oscillator strength at higher scattering angles. On the other hand, through comparison with the noninteracting cross sections we found that the lower lying spin wave seems less affected by scattering angle.

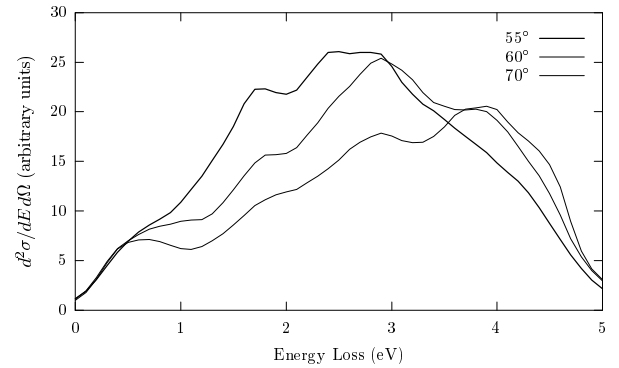


FIG. 7. Total cross sections for angles of incidence 55° , 60° and 70° . The main peak shifts toward higher energies according to the weight the different interband excitations gain or lose because of umklapp processes and according to which Stoner peaks are approached. Broadness increases with peak shift. Also, the higher optical mode clearly loses strength with increasing scattering angle, while the lower lying mode seems less affected.

IV. DISCUSSION

We wish to discuss some of the issues considered in this work pertaining to other theoretical and experimental findings. First of all, as we have shown (cf. Fig. 2(b)), the maximum in the SPEELS spectrum does not necessarily correspond to the exchange splitting energy of the ferromagnet, since the peak is at 3 eV and $\Delta = 2$ eV in our model. Thus, the common assumption that this peak allows us to estimate the magnetic moment [22,23] through its correlation with exchange splitting should be reconsidered, both in bulk and surface studies.

Also, the broadness of the spectrum is generally associated with a non constant exchange splitting over the Brillouin zone. While we agree a non constant exchange splitting will have this effect, we have seen that a most important source of broadness is umklapp scattering, together with the structure of the interband densities of Stoner states of the material. In particular, even for specular or near specular scattering, will a model with rigidly split bands present a relatively broad spectrum. Still, according to our interband densities of Stoner states plot, for rigidly split bands we expect to see a maximum at exchange splitting. Unfortunately there are no reliable results for specular scattering in the case of Fe. [39] In this regard, the case of Ni would be very interesting to investigate in more detail. To begin with, the results of Kirschner, Rebenstorff, and Ibach [11] and of Abraham and Hopster [13] are contradictory. Indeed, the former reported a broad maximum around exchange splitting for near specular scattering, while the latter stated that they see no sharp feature at that energy. According to our picture, Abraham and Hopster's result would be explained only if the matrix elements $W_{nn'}$ are always weak for energies near exchange splitting. An accurate calculation of the interband densities of Stoner states and of the weights $W_{nn'}$ would be most clarifying in this respect. For off specular scattering, however, both groups reported a weak dependence on scattering angle. This is plausible, according to our results. In Fig. 6 we see that the $\langle |W_{nn'}|^2 \rangle$ may remain relatively unchanged for certain scattering angle intervals, with, consequently, little change in the SPEELS spectra.

As mentioned in the introduction, moreover, Abraham and Hopster interpret the onset of Stoner excitations found in their work in terms of the $3d$ band structure of Ni. Again, this could readily be verified having at hand the interband densities of Stoner states for this material. Indeed, these authors consider in particular interband excitations corresponding to $nn' = 55$, the onset of which, if they exist, could be easily identified in a graph like that in Fig. 3(a). A point still to be verified would be if the matrix elements for such excitations are sufficiently important.

Spin waves, both acoustic and optical, have long been predicted in itinerant ferromagnets and subsequently observed through neutron scattering. [1,4,9] The question

is, then, if these are observable in SPEELS. The question to be studied in the future is if there can be enough coupling between the incoming electron and those in the solid to excite an optical spin wave. In our model, it is umklapp processes that provide optical spin waves with the necessary oscillator strength to contribute significantly to the spectra. It could be, however, the acoustic waves, when present, drain most of the oscillator strength. This is plausible because it is known that acoustic spin waves in Fe arise upon hybridization of d electrons with sp electrons. Matrix elements with sp hybridization will be more important because of the larger s wave functions. This implies, of course, as our model does, that optical modes are mainly d in character. The case of Ni appears again to be different, since even a pure d band model of Ni shows acoustic spin waves. [5]

The analysis presented in this work can prove useful more broadly in the understanding of ferromagnetism. Recently, Hirsch has presented a model of ferromagnetism without exchange splitting, in which spin polarization arises upon broadening of the spin-up bands relative to spin-down. [40] If this mechanism plays an important role in itinerant ferromagnets, then the interband densities of Stoner states will change considerably because other pairs of bands will be involved than those in the Stoner picture of ferromagnetism. Consequently, the predicted exchange scattering spectra will be different in both pictures. Thus SPEELS can prove a useful tool to validate or disprove Hirsch's model, possibly improving resolution previously.

Finally, we would like to comment on the bulk *vs.* surface question. Our calculations here have focused on bulk properties. However, some authors have presented SPEELS as a technique more appropriate for surface studies. [23,25] The reason is concern regarding the mean free path of electrons at the energies used in SPEELS. The question raised, however, is not simple and requires more detailed consideration, both theoretically and experimentally. Still, most of the observations to date have been discussed in the light of bulk calculations. [12,13,20] In this regard, a recent report on the electron dynamics at the surfaces of noble metals (Ag and Cu) is appropriate to mention. Bürgi *et al.* [41] have found that the dynamics of hot electrons at surfaces can be dominated by bulk electrons. This offers more support to the premise that our results offer a sensible explanation for SPEELS results.

V. SUMMARY AND CONCLUSIONS

In this work we address the problem of the interpretation of the SPEELS spectrum of itinerant ferromagnets. We find that considerably more information can be drawn from these measurements than has been recognized until now. We have found that the peaks of the spectra in the Stoner region are the image of a few interband

densities of Stoner states of the material. These are very sensitive to the electronic structure of the material and illustrate very clearly the allowed and forbidden interband excitations. The important band couples in SPEELS are determined by the average weight of the squared matrix elements of the pendant Stoner excitations. In this respect, umklapp processes play a most fundamental role. Our model also predicts that optical spin waves should be excited in SPEELS experiments, with umklapp scattering providing the necessary oscillator strength. Our results allow us also to explain several of the features observed in SPEELS spectra. From the theoretical point of view, *ab initio* calculations of the interband densities of Stoner states and matrix elements $W_{nn'}$ would provide closer look to the details of the mechanisms behind SPEELS. The differences between different ferromagnets, like Fe and Ni, could also be better understood. From the experimental point of view, measurements with higher resolution would be desirable, particularly for the detection of spin waves. We think our results provide a good starting point for those further studies.

ACKNOWLEDGMENTS

R.S. would like to thank the members of the Department of Applied Physics at Chalmers University of Technology for their hospitality during a stay in which part of this work was done. This project was supported by the Swedish Natural Science Research Council. R.S. would also like to thank Suk Joo Youn and Ove Jepsen for LMTO-ASA data for Fe, and Anthony Paxton for providing him with useful literature. Many thanks in particular to Prof. A. J. Freeman for encouraging discussions.

[1] R. Kubo, T. Izuyama, D. J. Kim, and Y. Nagaoka, **17** Suppl. B-I, 67 (1962); T. Izuyama, D. J. Kim, and R. Kubo, *J. Phys. Soc. Jpn.* **18**, 1025 (1963).
[2] C. Herring, in *Magnetism*, Vol. IV, edited by G. T. Rado and H. Suhl (Academic Press, New York, 1966).
[3] H. A. Mook, R. M. Nicklow, E. D. Thompson, and M. K. Wilkinson, *J. Appl. Phys.* **40**, 1450 (1969).
[4] H. A. Mook and R. M. Nicklow, *Phys. Rev. B* **1**, 336 (1973).
[5] R. D. Lowde and c. G. Windsor, *Adv. Phys.* **19**, 813 (1970).
[6] J. F. Cooke, *Phys. Rev. B* **7**, 1108 (1973).
[7] J. F. Cooke, J. W. Lynn, and H. L. Davis, *Phys. Rev. B* **21**, 4118 (1980).
[8] H. Tang, M. Plihal, and D. L. Mills, *J. Magn. Magn. Mater.* **187**, 23 (1998).
[9] T. G. Perring, A. T. Boothroyd, D. McK. Paul, A. D.

Taylor, R. Osborn, R. J. Newport, J. A. Blackman, and H. A. Mook, *J. Appl. Phys.* **69**, 6219 (1991).
[10] H. Hopster, R. Raue, and R. Clauber, *Phys. Rev. Lett.* **53**, 695 (1984).
[11] J. Kirschner, D. Rebenstorff, and H. Ibach, *Phys. Rev. Lett.* **53**, 698 (1984).
[12] D. Venus and J. Kirschner, *Phys. Rev. B* **37**, 2199 (1988).
[13] D. L. Abraham and H. Hopster, *Phys. Rev. Lett* **62**, 1157 (1989).
[14] S. Yin and E. Tosatti, ICTP, Trieste. Preprint IC/81/129.
[15] J. Glazer and E. Tosatti, *Solid State Commun.* **52**, 905 (1984).
[16] G. Vignale and K. S. Singwi, *Phys. Rev. B* **32**, 2824 (1985).
[17] C. J. Bocchetta, E. Tosatti, and S. Yin, *Z. Phys. B* **67**, 89 (1987).
[18] R. Saniz and S. P. Apell, *Phys. Rev. B* **48**, 3206 (1993).
[19] M. Plihal and D. L. Mills, *Phys. Rev. B* **58**, 14407 (1998).
[20] M. Plihal, D. L. Mills, and J. Kirschner, *Phys. Rev. Lett.* **82**, 2579 (1999).
[21] J. Kirschner and J. Hartung, *Vacuum* **41**, 491 (1990).
[22] T. G. Walker, A. W. Pang, H. Hopster, and S. F. Alvarado, *Phys. Rev. Lett.* **69**, 1121 (1992).
[23] H. Hopster, *Surf. Rev. Lett.* **1**, 89 (1994).
[24] M. P. Gokhale, A. Ormeci, and D. L. Mills, *Phys. Rev. B* **46**, 8978 (1992).
[25] M. P. Gokhale and D. L. Mills, *Phys. Rev. B* **49**, 3880 (1994).
[26] M. Plihal and D. L. Mills, *Phys. Rev. B* **52**, 12813 (1995).
[27] A similar claim was made in Ref. [11].
[28] A. L. Fetter and J. D. Walecka, *Quantum Theory of Many-Particle Systems* (McGraw-Hill, New York 1971).
[29] J. S. Griffith, *The Theory of Transition-Metal Ions*, (Cambridge, Cambridge, 1961).
[30] N. W. Ashcroft and N. D. Mermin, *Solid State Physics* (Saunders College, Philadelphia, 1976).
[31] This is a FPLMTO estimate of the majority *d*-bandwidth for Fe at the *H* point. R. Saniz (unpublished).
[32] The value of the effective intra-atomic Coulomb interaction is found to be around 0.5 to 1 eV for all transition metals. See E. P. Wohlfarth, in *Ferromagnetic materials*, Vol. 1, edited by E. P. Wohlfarth (North-Holland, Amsterdam, 1980). See also G. Tréglia, F. Ducastelle, and D. Spanjaard, *J. Physique* **43**, 341 (1982), and M. M. Steiner, R. C. Albers, and L. J. Sham, *Phys. Rev. B* **45**, 13272 (1992).
[33] An LMTO-ASA estimation gives approximately 36% for the polarization of *d* electrons. S. J. Youn (private communication).
[34] The LMTO-ASA value is roughly 0.09 states/eV·atom. S. J. Youn and O. Jepsen (private communications).
[35] Interesting references in the case of Ni for this difficult question are H. I. Starnberg and P. O. Nilsson, *J. Phys. F: Met. Phys.* **18**, L247 (1988), and F. Aryasetiawan, *Phys. Rev. B* **46**, 13051 (1992). See also F. Aryasetiawan and O. Gunnarsson, *Rep. Prog. Phys* **61**, 237 (1998), for a more general discussion.
[36] Note that the densities of Stoner states do not quite vanish for zero energy loss. For off specular scattering, $E = 0$

corresponds to elastic scattering with finite momentum transfer, which presents a low but finite density of Stoner states.

- [37] Indeed, it is not difficult to see that for $n = 3, 4, 5$ the Stoner peaks correspond essentially to excitations coupling (minority) antibonding holes to (majority) antibonding electrons, for lower energy cases, and to bonding electrons for higher energy. The same is true for the coupling of the $n = 1, 2$ bonding holes with electrons.
- [38] See R. B. Muniz, J. F. Cooke, and D. M. Edwards, J. Phys. F: Met. Phys. **15**, 2357 (1985). This is probably also why we find the optical mode contribution at too high an energy (just below 2 eV) with respect to e.g. the dynamical susceptibility result in Ref. [7], which yields a value below 400 meV. Although both results cannot be directly compared because they correspond to momenta of different magnitude and in different directions, it is unlikely that the dispersion relation can change so much.
- [39] The measurements of Venus and Kirschner in Ref. [12] show no peak around exchange splitting for specular scattering, but the authors warn their results in that case are not reliable.
- [40] J. E. Hirsch, Phys. Rev. B **59**, 6256 (1999).
- [41] L. Bürgi, O. Jeandupeux, H. Brune, and K. Kern, Phys. Rev. Lett. **82**, 4516 (1999).